Received: 15 Mar 2022 | **Accepted:** 23 Jan 2023 **Genel Tıp Derg. Volume** 33/**Issue** 1 (February), 14-20
DOI: 10.54005/geneltip.1088311

ORIGINAL ARTICLE

Nephroprotective Effect of Astaxanthin Against Radiotherapy Via TAS, TOS (Biochemical), TNF-*a*, CASPASE-3 (Immunohistochemical), SIRT-1-P53 (Molecular) Pathway in Rats

Astaksantin'in Sıçanlarda TAS, TOS (Biyokimyasal), TNF-*a*, CASPASE-3 (İmmünohistokimyasal), SIRT-1-P53 (Moleküler) Yolu Aracılığıyla Radyoterapiye Karşı Nefroprotektif Etkisi

[1]Gamze Erkilinç, [2]Mehmet Bedir, [3]Leyla Elif Özgü Ayözger, [4]Hatice Kübra Doğan, [5]Nasif Fatih Karakuyu

[1] Urla State Hospital, Department of Medical Pathology
[2] Süleyman Demirel University Faculty of Medicine, Department of Medical Biochemistry
[3] Burdur Mehmet Akif Ersoy University Faculty of Veterinary Medicine, Department of Veterinary Pathology
[4] Süleyman Demirel University, Graduate School of Natural and Applied Sciences, Department of Bioengineering
[5] Süleyman Demirel University Faculty of Medicine, Department of Medical Pharmacology

Correspondence

Gamze Erkilinç, Urla Devlet Hastanesi, Tıbbi Patoloji Bölümü

E-Mail: gamzecirak@gmail.com

How to cite ?

Erkılınç G. , Bedir M. , Ayözger L. E. Ö. , Doğan H. K. , Karakuyu N. Nephroprotective Effect of Astaxanthin Against Radiotherapy Via TAS, TOS (Biochemical), TNF-a, CASPASE-3 (Immunohistochemical), SIRT-1-P53 (Molecular) Pathway in Rats. Genel Tıp Dergisi. 2023; 33(1): 14-20.

ABSTRACT

Aim: To evaluate the effects of Astaxanthin (ATX), known for its antioxidant properties, on the kidneys of rats given radiation by biochemical measuring total oxidant level (TOS), total antioxidant level (TAS), immunohistochemically by Cas3 (Cysteine Aspartate Specific ProteASEs), TNF-a (Tumor necrosis factor-alpha), and molecularly by P53, SIRT (Sirtuin -1) pathways.
Materials and Methods: The rats were divided into 4 groups (8 rats per group): control, radiotherapy (RT), RT+ATX, ATX. ATX was given to rats at 4 mg/kg for 7 days. We evaluated to effect of ATX in rats' kidneys damaged by RT by comparing all groups with TAS, TOS, Cas 3, TNF-a, and SIRT-1, P53.
Results: TAS levels were similar among the control, RT, RT+ATX, and ATX groups. TOS levels were significantly lower in the ATX group compared to RT, Control, and RT+ATX groups. Histopathologically marked hyperemia and in some kidneys, small hemorrhages were observed in the RT group. In addition, marked glomerular sclerosis was also detected in this group. With ATX, we observed significant improvement in the RT+ATX group. Immunohistochemically revealed increased Cas3 expressions, tubular cells in TNF-a expressions in the RT group. ATX treatment decreased Cas3 and TNF-a expression in the RT+ATX group. No Cas3 and TNF-a expression was observed in both control and ATX groups. There was no significant difference between the groups in SIRT-1, P53 values.
Conclusion: It was observed that Astaxanthin is a carotenoid that may benefit the recovery of tubular and glomerular cells in kidney damage after radiation, and it has positive effects on oxidative stress.

Key words: Radiotherapy effects, Rat kidney, Astaxanthin, Caspase 3, SIRT-1, P53, TNF-a

ÖZ

Amaç: Antioksidan özelliği ile bilinen Astaksantin'in (ATX) radyasyon verilen sıçanların böbrekleri üzerindeki etkilerini biyokimyasal olarak total oksidan düzeyi (TOS), total antioksidan düzeyi (TAS), Cas3 (Sistein Aspartat Spesifik ProteASE'ler), TNF-a (Tümör nekroz faktörü-alfa) ile immünohistokimyasal olarak ve P53, SIRT (Sirtuin -1) yolakları ile moleküler olarak değerlendirmek.
Gereç ve Yöntem: Sıçanlar 4 gruba ayrıldı (grup başına 8 sıçan): kontrol, radyoterapi (RT), RT+ATX, ATX. Sıçanlara 7 gün boyunca 4 mg/kg ATX verildi. RT ile hasar görmüş sıçanların böbreklerinde ATX'in etkisini tüm gruplarda TAS, TOS, Cas 3, TNF-a ve SIRT-1, P53 ile karşılaştırarak değerlendirdik.
Bulgular: TAS düzeyleri kontrol, RT, RT+ATX ve ATX grupları arasında benzerdi. TOS seviyeleri, ATX grubunda RT, Kontrol ve RT+ATX gruplarına kıyasla anlamlı derecede düşüktü. RT grubunda histopatolojik olarak belirgin hiperemi ve bazı böbreklerde küçük kanamalar gözlendi. Ayrıca bu grupta belirgin glomerüler skleroz da saptandı. ATX ile, RT+ATX grubunda belirgin şekilde iyileşme gözlemledik. İmmünohistokimyasal olarak RT grubunda Cas3 ekspresyonlarında artış, TNF-a'nın tübüler hücreler ekspresyonu saptandı. ATX tedavisi, RT+ATX grubunda Cas3 ve TNF-a ekspresyonunu azalttı. Hem kontrol hem de ATX gruplarında Cas3 ve TNF-a ekspresyonu gözlenmedi. SIRT-1, P53 değerlerinde gruplar arasında anlamlı fark yoktu.
Sonuç: Astaksantin'in radyasyon sonrası böbrek hasarında tübüler ve glomerüler hücrelerin iyileşmesine fayda sağlayabilecek bir karotenoid olduğu ve oksidatif stres üzerinde olumlu etkileri olduğu gözlendi.

Anahtar Kelimeler: Radyoterapi etkileri, Rat böbreği, Astaksantin, Kaspaz 3, , Kaspaz 3, SIRT-1, P53, TNF-a

Introduction

Damage due to radiotherapy; It is a complex series of processes that resembles the healing of traumatic wounds and affects the entire cell inside and outside of the irradiated area, the effect of which can continue for many years. Cellular damage, ongoing repair, inflammation and many pathophysiological events are triggered in each fraction. Exposure to ionizing radiation not only causes DNA damage, but also causes a burst of free radicals that alter proteins, carbohydrates, and lipids (1).

After physical trauma, cytokines such as TNF-a (Tumor necrosis factor-alpha), IL-1 (interleukin-1), IL-8 (interleukin-8), which are pro-inflammatory cytokines, are released (1, 2). TNF-a is a proinflammatory cytokine that triggers apoptosis and inflammation (3). This cytokine, which is effective in the inflammatory response, can be used as a marker in experimental models. In the study investigating the effect of cisplatin on nephrotoxicity, it was observed that the TNF-a level increased in the early period of renal damage (4).

Peer-Review: Double anonymized - Two External
Plagiarism Checks: Yes - Turnitin
Complaints: geneltip@selcuk.edu.tr

As a result of the release of various cytokines; gene expression changes are observed in signaling pathways related to the production of hormones and growth factors (5). At the molecular level, P53 block occurs in normal cells after radiation in G1 phase (5). P53 becomes stable and accumulates in the nucleus. It prolongs the half-life, binds to specific parts of the DNA, inhibits the cell cycle in the G1 phase, allowing the cell to gain time for repair. In the absence of a growth factor in the damaged cell, these cells go to apoptosis. With the post-transcriptional increase of the P53 protein, increasing growth factors and special receptors encoded by protooncogenes to be effective provide signal transmission and control in the cell (6). Caspases (Cysteine Aspartate Specific ProteASEs) are inactive cysteine-protease group enzymes and play an important role during apoptosis via activated in various ways (7).

Sirtuin-1 (SIRT-1) is one of the positive regulators of autophagy (8). SIRT-1 is a nicotinamide adenosine dinucleotide-dependent deacetylase enzyme (8). There is an extensive list of SIRT-1 substrates that are constantly increasing and contain many transcription factors such as nuclear factor kappa B (9). Besides the anti-inflammatory effects of SIRT-1, cytoprotective effects have also been reported (10).

Astaxanthin (ATX), known for its antioxidant properties in recent years, is a fat-soluble xanthyl group carotenoid pigment found naturally in a wide variety of plants and algae and in living things such as salmon, crabs, and shrimp (11). The conjugated double bond in the middle of the compound gives ATX its red color (12). The antioxidant effect of ATX is in two ways; it scavenges free radicals, protects against chain reactions that free radicals cause, and terminates chain reactions (13). Unlike carotenoids, ATX is a stronger antioxidant because it contains oxygen groups. (14). The effects of ATX on the liver, brain, cardiovascular organs were investigated (15). Since it contains hydroxyl-keto groups in its ATX structure, it adapts well to the cell membrane and provides a more permanent effect on both the inner and outer membranes of the cell than other carotenes (16). ATX has been approved by the FDA (Food and Drug Administration) (17).

Oxidative damage can be determined by measuring serum concentrations of different antioxidants. However, these measurements require time-consuming, costly, and complex techniques, and it is not practical to measure different antioxidant molecules separately. Therefore, measuring total oxidant level (TOS) and total antioxidant level (TAS) is more effective in determining oxidative damage (18).

It has been shown in the studies on kidney-related ATX that treatment with ATX improves kidney functions in diabetic rats, reduces renal damage (19).Also ATX has an anti-inflammatory activity in kidney diseases (20), and anti-inflammatory activity on eyes and skin against the harmful effects of radiation (21). In addition, it has been reported that ATX has effects in protecting cells and organs in reperfusion-induced oxidative stress induced by SIRT-1, P53, SIRT1/FOXO3 (22).

Based on this information, we aimed to investigate the efficacy of ATX biochemically with TAS, TOS, immunohistochemically with Cas 3, TNF-a, and P53, SIRT-1 pathways molecularly in the kidneys of rats which received radiotherapy.

Materials and Methods

Study animals and design of experiment

The animal studies were approved by Suleyman Demirel University's local animal ethics council (Ethic no: 2020-07/06), and this study was funded by Suleyman Demirel University's Scientific Research Projects Coordination Unit under project number TSG-2020-8134. The study was carried out in conformity with the ARRIVE 2.0 criteria (Animal Research: Reporting in Vivo Experiments). The study involved 32 Wistar albino rats collected from the SDU Experimental Animals Laboratory, all of which were adult females weighing 250-300 g. They were kept at 21–22 °C and 60% humidity, with a 12 h light:12 h dark cycle, and were given normal commercial chow (Korkuteli Yem, Antalya, Türkiye), with food and water available ad libitum in the same cage settings. The rats in the study were divided into four groups, each with eight rats: control, RT, RT+ATX, and ATX. The rats in all groups were brought to the place where the radiation apparatus was located under the same settings on the first day of the trial. Although only the RT and RT+ATX groups were irradiated, 90 mg/kg ketamine and 10 mg/kg xylazine were administered intraperitoneally for anesthesia to ensure that all animals were treated equally. One ml of saline solution was given to the control group apart from i.p. anesthesia for 7 days. The irradiation procedure of the rats was performed by a radiation oncologist and medical physicist in the radiation oncology department of our institute. Under anesthesia, a single dose of 8 Gy X-Ray renal radiotherapy was administered to the radiotherapy group. All rats in the RT group were given 1 ml of saline solution for 7 days. A single dose of 8 Gy X- Ray and 1ml of 4 mg/kg ATX were administered orally under anesthesia to the RT+ATX group. Oral 1ml of 4mg/kg ATX was administered for 7 days to the ATX group.

Renal regions were designated with a marker on the thigh surfaces, and the marked point was exposed to radiation. A 6 MV x-ray beam and the Anisotropic Analytical Algorithm dose calculation algorithm were performed and 8 Gy of irradiation was prescribed. The room temperature was 22 degrees during the irradiation.

Incision, tissue storage and evaluation

Sedation was achieved with 80-100 mg/kg Ketamine and 8-10 mg/kg Xylazine 24 hours after the end of the experiment. Renal tissue samples were divided into two pieces. Tissues for biochemical and genetic analysis were collected and preserved at -20° C. Tissues for

histopathological and immunohistochemical analyses were placed in 10% formaldehyde.

Measurement of oxidative stress parameters

For oxidant-antioxidant analysis, renal tissue samples were homogenized with an Ultra Turrax Janke&Kunkel T-25 homogenizer (IKA®-Werke, Germany). Total antioxidant status (TAS), total oxidant status (TOS), and OSI were assessed spectrophotometrically (Beckman Coulter AU 5800, Beckman Coulter, USA) with commercial kits (Rel Assay Diagnostics, Gaziantep, Türkiye) and computed using the formula. Antioxidants in the sample converted the dark blue-green 2,2'-Azino-bis (3-ethylbenzothiazoline-6-sulfonic acid) (ABTS) radical to the colorless reduced ABTS form for TAS measurement. The change in absorbance at 660 nm is proportional to the sample's total antioxidant content. The antioxidative impact of the sample against the powerful free radical reactions triggered by the generated hydroxyl radicals was determined using this approach. The data are given in milliliters of Trolox equivalent per liter (23).

Oxidants in the sample oxidized the ferrous ion-dianisidine complex to the ferric ion for TOS analysis. Glycerol molecules, which were plentiful in the reaction media, promoted oxidation processes. In an acidic media, the ferric ion formed a colorful complex with xylenol orange. The color intensity, which could be measured spectrophotometrically, was related to the total amount of oxidant molecules that were already present in the sample. The assay was calibrated with hydrogen peroxide, and the results were expressed in terms of micromolar hydrogen peroxide equivalent per liter (μmol H2O2 Eqv/L)(24).

Histopathological evaluation

During the necropsy, kidney samples were gently removed and fixed in 10% neutral formalin solution. After two-day fixation, tissue samples were routinely processed by an automatic tissue processor (Leica ASP300S, Wetzlar, Germany) and embedded in paraffin wax. After cooling the paraffin blocks, 5 μm thickness sections were taken by a rotary microtome (Leica RM2155, Leica Microsystems, Wetzlar, Germany). Then, the sections were stained with hematoxylin-eosin (H&E), coverslip, and examined under a light microscope.

Immunohistochemical evaluation

For immunohistochemical examination 2 series of sections taken from all blocks of the kidneys drawn on poly-L-lysine coated slides were stained immunohistochemically for caspase-3 (Anti-caspase-3 Antibody (E-8): sc-7272) and TNF-a (Anti-TNFa Antibody (52B83):sc-52746, 1/100 dilution) Santa Cruz (Texas, USA) expression by streptavidin-biotin technique according to manufacturer instruction. The sections were incubated with the primary antibodies for a period of 60 min, and immunohistochemistry was carried out using biotinylated secondary antibody and streptavidin-alkaline phosphatase conjugate. EXPOSE Mouse and Rabbit Specific HRP/DAB Detection IHC kit (ab80436) (Abcam, Cambridge, UK) were used as secondary antibody. Diaminobenzidine (DAB) was used as the chromogen. For negative controls, antigen dilution solution was used instead of primary antibody. All examinations were performed on blinded samples by a pathologist.

For immunohistochemical analysis, sections were separately investigated for each antibody. To evaluate the severity of the immunohistochemical reaction of cells with markers, semiquantitative analysis was performed using a grading score ranging from (0) to (3) as follows: (0) = negative, (1) = focal weak staining, (2) = diffuse weak staining, (3) = diffuse strong staining. For evaluation, 10 different areas under 40X objective magnification in each section were examined. Morphometric analyses and microphotography were performed using the Database Manual Cell Sens Life Science Imaging Software System (Olympus Co., Tokyo, Japan). The results were saved and statistically analyzed.

Quantitative reverse transcription-polymerase chain reaction (RT-qPCR)

RNA isolation, cDNA synthesis and RT-qPCRs

Reverse transcription-polymerase chain reaction (RT-qPCR)

Total RNA was isolated from rat tissues using the TRIzolTM Reagent (Invitrogen), as directed by the manufacturer. A MySPEC microvolume spectrophotometer was used to determine RNA concentration and purity (VWR). Using oligo dT primers, 1 ug RNA was reverse transcribed using the iScript cDNA Synthesis kit (Bio-Rad Laboratories, Hercules, CA). The reaction mixture was incubated for 5 minutes at 25°C, 20 minutes at 46°C, and 1 minute at 95°C. The iTaq Universal SYBR Green Supermix (Bio-Rad Laboratories, Hercules, CA) was used for real-time PCR amplification, and the fluorescence signal was measured using a CFX96 instrument (Bio-Rad Laboratories, Hercules, CA). To amplify, specific primers were created. SIRT-1 (Forward 5'-CCTCTAGTTCCTGTGGCAGTA-3', Reverse 5' CGGTCTGTCAGCATCATCTTC-3'), For each PCR, P53 (Forward 5'-CGGCTCCGACTATACCACTAT-3', Reverse 5'-TGTCCCGTCCCAGAAGATT-3'). cDNA samples were examined in triplicate. GAPDH (Forward 5'-CAAGGTCATCCCAGAGCTGAA-3', Reverse 5'-CATGTAGGCCATGAGGTCCAC-3') expression was used for normalization. The following PCR conditions were used: 10 minutes of denaturation at 95 °C, followed by 40 cycles of 10 seconds at 95 °C and 30 seconds at 60 °C. The entire reaction volume was 25l, and the template was 100ng cDNA. The comparative Ct method was used to provide the relative measurement of gene expression. All results were presented in the graph as a fold change.

Statistical Analysis

For statistical analysis, of scores of the groups were compared between the groups for this purpose, the Oneway ANOVA Duncan test was used by the SPSS-22.00 package program. The level of significance was considered as $P < 0.05$.

Results

Biochemical findings

TAS levels were similar among the control, RT, RT+ATX, and ATX groups. TOS levels were significantly lower in the ATX group compared to RT, Control and RT+ATX groups. Figure 1A shows TAS levels and figure 1B shows TOS levels among the groups. Mean levels of TAS and TOS are shown in Table 1.

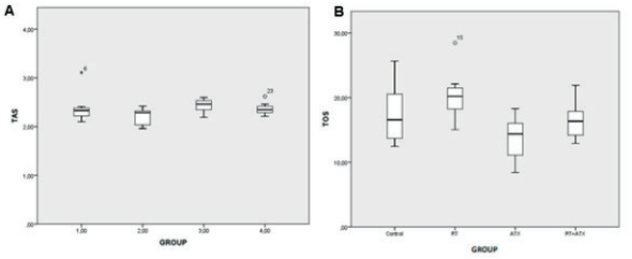

Figure 1. A: TAS levels among the groups,.B: TOS levels among the groups.

TAS: Total antioxidant status, TOS: total oxidant status, RT: radiotherapy, ATX: Astaxanthin

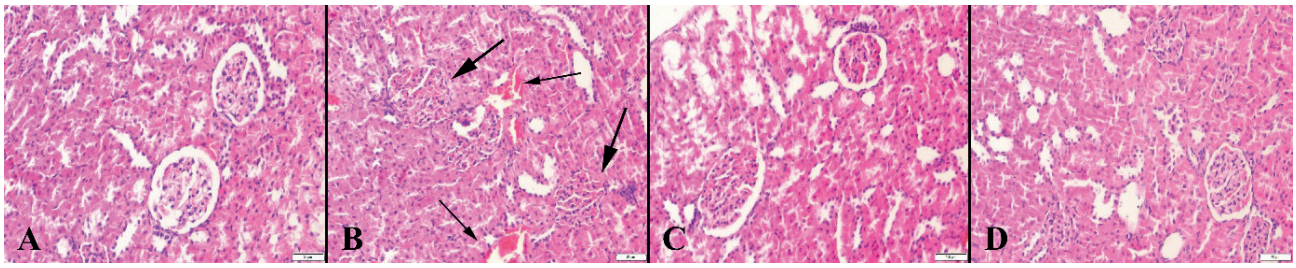

Figure 2. Kidney appearance between the groups. (A) Normal tissue histology in the control group. (B) Marked hyperemia (thin arrows) and glomerulosclerosis (thick arrows) in the RT group. (C) Almost normal appearance in the RT+ATX group (D) Normal tissue histology in the ATX group, (H&E x200), Bar=50µm. RT: radiotherapy, ATX: Astaxanthin

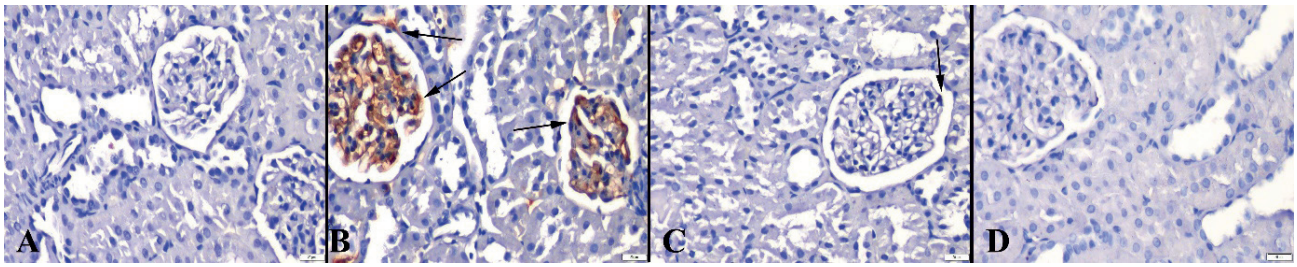

Figure 3. Caspase-3 immunohistochemistry findings among the group (x200). (A) Negative expression in the control group, (B) Marked increase in glomerular cells (arrows) in RT group, (C) decreased increase (arrow) in glomerular cells in RT+ATX group, (D) No expression in ATX group, Streptavidin biotin peroxidase method, Bars=20µm. RT: radiotherapy, ATX: Astaxanthin

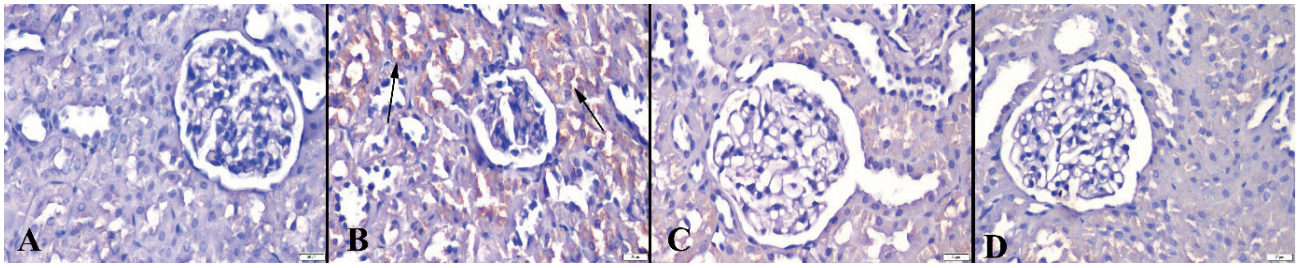

Figure 4. TNF-a expressions among the groups (x200). (A) No expression in the control group. (B) Increased expressions in tubular cells (arrows) in the RT group. (C) Decreased expressions in the RT+ATX group. (D) Negative immunoexpressions in ATX group, Streptavidin biotin peroxidase method, Bars=20µm.

TNF-a: Tumor necrosis factor-alpha, RT: radiotherapy, ATX: Astaxanthin

Table 1. Statistical analysis result of mean levels of TAS and TOS between the groups

	Control	RT	ATX	RT+ATX	P value
TOS	17.5±4.9	20.4±3.9	13.6±3.8	16.4±2.9	0.029
TAS	2.3±0.3	2.2±0.1	2.4±0.1	2.3±0.1	0.111

TAS: Total antioxidant status, TOS: total oxidant status, RT: radiotherapy, ATX: Astaxanthin

Histopathological findings

Histopathological examination of the kidneys revealed normal tissue architecture in the control group. Marked hyperemia and in some kidneys, small hemorrhages were observed in the RT group. In addition, marked glomerular sclerosis was also detected in this group. ATX treatment markedly ameliorated in the RT+ATX group. NThere were no pathological findings in the ATX group (Fig.2).

Immunohistochemical findings

Immunohistochemical findings revealed increased Cas-3 expressions in the RT group. ATX treatment decreased expression in the RT+ATX group. No expression was observed in both control and ATX groups (Fig.3).

The examination of TNF-a expressions between the groups revealed increased expressions in tubular cells RT group. ATX treatment markedly decreased expressions in the RT+ATX group. No TNF-a expressions occured in control and ATX groups (Fig.4). Statistical analysis results of immunohistochemical scores are shown in Table 2.

Table 2. Statistical analysis result of immunohistochemical scores between the groups.

Groups	Cas-3 Scores	TNF-a Scores
Control	0.14±0.14^{a}	0.14±0.14^{a}
RT	2.14±0.69^{b}	1.42±0.53^{b}
RT+ATX	0.42±0.20^{a}	0.57±0.53^{a}
ATX	0.14±0.14^{a}	0.14±0.14^{a}
P value	< 0.001	< 0.001

*: The differences between the means of groups carrying different letters between the groups are statistically significant, P<0.001.

**: Data expressed mean ± standard deviation (SD). One-way ANOVA Duncan test.

This study results indicated that RT causes damage in kidneys, ATX treatment ameliorated pathological findings. Cas 3: Cysteine Aspartate Specific ProteASEs, TNF-a: Tumor necrosis factor-alpha, RT: radiotherapy, ATX: Astaxanthin

Genetic Findings

SIRT-1 and P53 levels were similar among the groups. Figure 5A shows SIRT-1 and figure 5B shows P53 levels among the groups. Table 3 shows the comparison of the SIRT 1 and P53 levels among the groups.

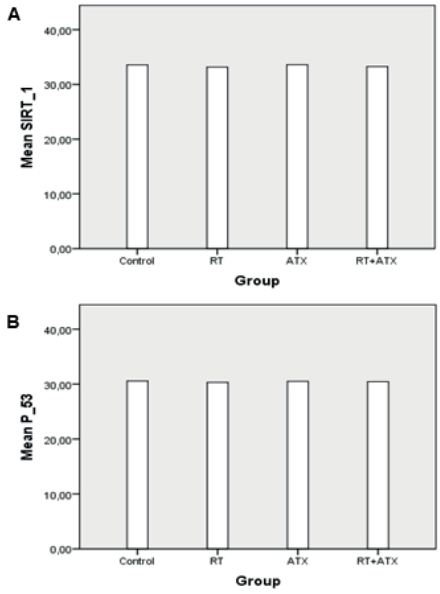

Figure 5. A: SIRT-1 levels among the groups, B: P 53 levels among the groups. SIRT-1: Sirtuin-1, RT: radiotherapy, ATX: Astaxanthin

Table 3. Statistical analysis result of genetic findings between the groups.

	Control	RT	ATX	RT+ATX	P value
SIRT-1	33.5±0.2	33.1±0.1	33.6±0.2	33.2±0.5	0.248
P-53	30.5±0.6	30.3±0.2	30.4±0.4	30.4±0.1	0.548

SIRT-1: Sirtuin-1, RT: radiotherapy, ATX: Astaxanthin

Discussion

In this study, the effects of ATX, which has antioxidant and anti-inflammatory properties, were investigated in rats with a radiotherapy-induced damage model in the kidney. It was determined that the administration of "1 ml of 4mg/kg ATX by oral gavage method for 7 days" together with 8 Gy X-ray dose radiotherapy had a positive effect on the kidney tissue.

Radiation-induced kidney glomerulosclerosis and/or tubulointerstitial fibrosis may cause serious damage. If 23 Gy dose is given for more than 5 weeks, the risk of kidney damage is high (25). More recently, a tolerance dose of 20 Gy has been proposed, therefore, it is seen that the incidence of radiation dose-related kidney damage has decreased (25). Radiation was proven to damage the kidney causing nuclear oxidation in glomeruli and tubule cells. This increase was more pronounced 4 weeks after the first irradiation and was found to continue up to 24 weeks (26). In our study, the control, RT, ATX+RT and ATX groups were given equal doses of radiation for the same duration, and glomerulosclerosis, significant hyperemia and small hemorrhage foci were observed in H&E stained

sections in the RT group. In this case, regardless of dose and duration, it supports the effect of radiation on the kidney.

Recently, many studies have been conducted on antioxidants, and it has been shown that lycopene, one of the antioxidants, has a protective effect on cisplatin-induced nephrotoxicity (27). In another study, it was found that foods such as soybean and sesame had a positive effect on cisplatin nephrotoxicity (28).

ATX has been shown to increase immune response and decrease inflammation (29). Furthermore antioxidant, neuroprotective, immunomodulatory and antidiabetic effects of ATX was shown in the literature

(30, 31). Mercury chloride, inorganic arsenic, colistin ATX has also been determined to have a protective effect on nephrotoxicity due to gentamicin (32). In our study we showed the beneficial effect of ATX to compansate radiotherapy induced renal toxicity when applied simultaneously with radiotherapy. Only in H&E stained sections, while significant hyperemia and glomerulosclerosis were observed in the RT group, we noticed that there was no significant RT effect in the ATX+RT group.

Superoxide dismutase and lipid peroxidase (MDA) levels were significantly decreased in the ATX group in rats which underwent ischemic reperfusion (I/R) in the kidney (15). In another study, TAS levels were higher and TOS, SOD (Superoxide dismutase) MDA values decreased significantly in the ATX+I/R group compared to the I/R group in rats administered I/R,(15). In our study, it was determined that TAS, was similar among the groups and TOS levels were significantly lower in the ATX group compared to RT, Control and RT+ATX groups.

To evaluate the inflammatory response in paracetamol-induced nephrotoxicity, its toxicity was investigated by analyzing the mRNA expressions of inflammatory cytokines TNF-a, IL-6 and IL-10. It was determined that inflammatory cytokines were decreased in the treated group (15). In the nephrotoxicity induced by cisplatin, TNF-a was higher in the toxicity group in the early period of renal damage compared to the treatment group (33). In our study, we observed that immunohistochemical expression of TNF-a was significantly higher in the renal tubule epithelium in the RT group compared to RT+ATX, ATX and control groups.

In another study investigating the effect of ATX on the PI3Akt signaling pathway, which plays an important role in antagonizing renal tubular apoptosis, the entire Bad/ Caspase signaling process. LY294002 pretreatment largely reversed the protective effect of ATX on renal tubular apoptosis after burns in rats, as well as the expression of signals in the mitochondrial-dependent pathway, which supported our deduction about the implication of the Akt/Bad/Caspase signaling cascade in the nephroprotection of ATX in early AKI secondary to severe burns (34). In our study, we observed that the immunohistochemical expression of Cas 3 was significantly higher in the kidney glomeruli cells in the RT group compared to the RT+ATX, ATX and control groups.

At the molecular level, many genes have been shown to be sensitive to radiation exposure (35). In the study investigating the role of the P53 gene following single and multiple radiation therapies, the group was injected with the vector containing the temperature-sensitive normal P53 gene in prostate cells and the other group was given multiple 2 Gy fractions against a single. When the P53 gene was functional, survival was observed to increase compared to the non-functional group (35). In contrast, another study reported that the mutated P53 gene in glioblastoma cells showed increased survival after multiple 2 Gy fractions compared to cells transfected with a normal P53 gene (36). In another study, it was found that each cell line in 8 types of radiosensitive tumors responded to fractionated radiation therapy independently of P53 (37). In our study, SIRT-1 and P53 levels were similar among the groups.

Conclusion: we concluded that Astaxanthin which is one of the important carotenoid, may have benefits on the recovery of tubular and glomerular cells in kidney damage after application of radiation, and has positive effects on suppressing oxidative stress.

Molecular markers including P53 and SIRT-1 were not affected by ATX in kidney of rats that received radiotherapy

Financial support: This study was supported by the Scientific Research Project Unit of Suleyman Demirel University (project code TSG-2020-8134).

Declarations of interest: None

References

1.Denham JW, Hauer-Jensen M. The radiotherapeutic injury–a complex 'wound'. Radiother Oncol. 2002;63(2):129-45.

2.Koj A. Termination of acute-phase response: role of some cytokines and anti-inflammatory drugs. General Pharmacology: The Vascular System. 1998;31(1):9-18.

3.Akbulut G, Dilek ON, Kahraman A, Köken T, Serteser M. The correlation between renal tissue oxidative stress parameters and TNF-alpha levels in an experimental model of ischemia-reperfusion injury in mice. Ulusal Travma Dergisi. 2005;11(1):11-6.

4.Carlos CP, Sonehara NM, Oliani SM, Burdmann EA. Predictive usefulness of urinary biomarkers for the identification of cyclosporine A-induced nephrotoxicity in a rat model. PLoS One. 2014;9(7):e103660.

5.Tsai M-H, Cook JA, Chandramouli GV, DeGraff W, Yan H, Zhao S, et al. Gene expression profiling of breast, prostate, and glioma cells following single versus fractionated doses of radiation. Cancer Res. 2007;67(8):3845-52.

6.Karaman A. Mide kanserinde P53 tümör supresör geninin rolü. Türkiye Klinikleri Tıp Bilimleri Dergisi. 2003;23:67-73.

7.Jahan S, Munawar A, Razak S, Anam S, Ain QU, Ullah H, et al. Ameliorative effects of rutin against cisplatin-induced reproductive toxicity in male rats. BMC Urol. 2018;18(1):1-11.

8.Kume S, Uzu T, Horiike K, Chin-Kanasaki M, Isshiki K, Araki S-i, et al. Calorie restriction enhances cell adaptation to hypoxia through Sirt1-dependent mitochondrial autophagy in mouse aged kidney. The Journal of clinical investigation. 2010;120(4):1043-55.

9.Salminen A, Kaarniranta K. SIRT1: regulation of longevity via autophagy. Cell Signal. 2009;21(9):1356-60.

10.Donmez G, Guarente L. Aging and disease: connections to sirtuins. Aging Cell. 2010;9(2):285-90.

11.Hussein G, Sankawa U, Goto H, Matsumoto K, Watanabe H. Astaxanthin, a carotenoid with potential in human health and nutrition. J Nat Prod. 2006;69(3):443-9.

12.Higuera-Ciapara I, Felix-Valenzuela L, Goycoolea F. Astaxanthin: a review of its chemistry and applications. Crit Rev Food Sci Nutr. 2006;46(2):185-96.

13.Chen Y, Li D, Lu W, Xing J, Hui B, Han Y. Screening and characterization of astaxanthin-hyperproducing mutants of Haematococcus pluvialis. Biotechnol Lett. 2003;25(7):527-9.

14.Shibata A, Kiba Y, Akati N, Fukuzawa K, Terada H. Molecular characteristics of astaxanthin and β-carotene in the phospholipid monolayer and their distributions in the phospholipid bilayer. Chem Phys Lipids. 2001;113(1-2):11-22.

15.Qiu X, Fu K, Zhao X, Zhang Y, Yuan Y, Zhang S, et al. Protective effects of astaxanthin against ischemia/reperfusion induced renal injury in mice. J Transl Med. 2015;13(1):1-9.

16.Mentese A, Turkmen S, Karaguzel E, Karaca Y, Tatli O, Sumer AU, et al. The predictive value of ischemia-modified albumin in long-term results of ischemia-reperfusion injury in an experimental testicular torsion model. Urology. 2012;80(3):689-94.

17.Inborr J, Lignell Å, editors. Effect of feeding astaxanthin-rich algae meal (Haematococcus pluvialis) on performance and carotenoid concentration of different tissues of broiler chickens. Proceedings of the XIII WPSA Conference on Poultry Meat Quality in Poznan (Poland: Session M1); 1997.

18.Erel O. A novel automated method to measure total antioxidant response against potent free radical reactions. Clin Biochem. 2004;37(2):112-9.

19.Chen Q, Tao J, Xie X. Astaxanthin promotes Nrf2/ARE signaling to inhibit HG-induced renal fibrosis in GMCs. Mar Drugs. 2018;16(4):117.

20.Chang MX, Xiong F. Astaxanthin and its effects in inflammatory responses and inflammation-associated diseases: recent advances and future directions. Molecules. 2020;25(22):5342.

21.Hagen C, Grünewald K, Xyländer M, Rothe E. Effect of cultivation parameters on growth and pigment biosynthesis in flagellated cells of Haematococcus pluvialis. Journal of Applied Phycology. 2001;13(1):79-87.

22.Gao D, Wang H, Xu Y, Zheng D, Zhang Q, Li W. Protective effect of astaxanthin against contrast-induced acute kidney injury via SIRT1-P53 pathway in rats. Int Urol Nephrol. 2019;51(2):351-8.

23.Erel O. A novel automated direct measurement method for total antioxidant capacity using a new generation, more stable ABTS radical cation. Clin Biochem. 2004;37(4):277-85.

24.Erel O. A new automated colorimetric method for measuring total oxidant status. Clin Biochem. 2005;38(12):1103-11.

25.Kunkler P, Farr R, Luxton R. The limit of renal tolerance to X rays. The British journal of radiology. 1952;25(292):190-201.

26.Robbins ME, Zhao W, Davis CS, Toyokuni S, Bonsib SM. Radiation-induced kidney injury: a role for chronic oxidative stress? Micron. 2002;33(2):133-41.

27.Atessahin A, Yilmaz S, Karahan I, Ceribasi AO, Karaoglu A. Effects of lycopene against cisplatin-induced nephrotoxicity and oxidative stress in rats. Toxicology. 2005;212(2-3):116-23.

28.Abdel-Wahab WM, Moussa FI, Saad NA. Synergistic protective effect of N-acetylcysteine and taurine against cisplatin-induced nephrotoxicity in rats. Drug Des Devel Ther. 2017;11:901.

29.Wang X, Zhao H, Shao Y, Wang P, Wei Y, Zhang W, et al. Nephroprotective effect of astaxanthin against trivalent inorganic arsenic-induced renal injury in wistar rats. Nutr Res Pract. 2014;8(1):46-53.

30.Ikeuchi M, Koyama T, Takahashi J, Yazawa K. Effects of astaxanthin in obese mice fed a high-fat diet. Biosci Biotechnol Biochem. 2007;71(4):893-9.

31.Naito Y, Uchiyama K, Aoi W, Hasegawa G, Nakamura N, Yoshida N, et al. Prevention of diabetic nephropathy by treatment with astaxanthin in diabetic db/db mice. Biofactors. 2004;20(1):49-59.

32.Ghlissi Z, Hakim A, Sila A, Mnif H, Zeghal K, Rebai T, et al. Evaluation of efficacy of natural astaxanthin and vitamin E in prevention of colistin-induced nephrotoxicity in the rat model. Environ Toxicol Pharmacol. 2014;37(3):960-6.

33.Cermik H, Taslipinar MY, Aydin I, Agilli M, Aydin FN, Ucar F, et al. The relationship between N-acetylcysteine, hyperbaric oxygen, and inflammation in a rat model of acetaminophen-induced nephrotoxicity. Inflammation. 2013;36(5):1145-52.

34.Guo S-X, Zhou H-L, Huang C-L, You C-G, Fang Q, Wu P, et al. Astaxanthin attenuates early acute kidney injury following severe burns in rats by ameliorating oxidative stress and mitochondrial-related apoptosis. Mar Drugs. 2015;13(4):2105-23.

35.Scott SL, Earle JD, Gumerlock PH. Functional P53 increases prostate cancer cell survival after exposure to fractionated doses of ionizing radiation. Cancer Res. 2003;63(21):7190-6.

36.Haas-Kogan DA, Kogan SS, Yount G, Hsu J, Haas M, Deen DF, et al. P53 function influences the effect of fractionated radiotherapy on glioblastoma tumors. International Journal of Radiation Oncology* Biology* Physics. 1999;43(2):399-403.

37.Dahlberg WK, Azzam EI, Yu Y, Little JB. Response of human tumor cells of varying radiosensitivity and radiocurability to fractionated irradiation. Cancer Res. 1999;59(20):5365-9.